



ELSEVIER

Mechanics Research Communications 31 (2004) 405–414

MECHANICS

RESEARCH COMMUNICATIONS

www.elsevier.com/locate/mechrescom

Continuum Dyson's equation and defect Green's function in a heterogeneous anisotropic solid [☆]

B. Yang ^{*}, V.K. Tewary

Materials Reliability Division, National Institute of Standards and Technology, Boulder, CO 80305, USA

Received 20 November 2003
Available online 10 December 2003

Abstract

A continuum Dyson's equation and a defect Green's function (GF) in a heterogeneous, anisotropic and linearly elastic solid under homogeneous boundary conditions have been introduced. The continuum Dyson's equation relates the point-force Green's responses of two systems of identical geometry and boundary conditions but of different media. Given the GF of either system (i.e., a reference), the GF of the other (i.e., a defect system with "defect" change of materials property relative to the reference) can be obtained by solving the Dyson's equation. The defect GF is applied to solve the eigenstrain problem of a heterogeneous solid. In particular, the problem of slightly inhomogeneous inclusions is examined in detail. Based on the Dyson's equation, approximate schemes are proposed to efficiently evaluate the elastic field. Numerical results are reported for inhomogeneous inclusions in a semi-infinite substrate with a traction-free surface to demonstrate the validity of the present formulation.

Published by Elsevier Ltd.

Keywords: Anisotropic elasticity; Dyson's equation; Eigenstrain; Green's function; Heterogeneity; Inhomogeneous inclusion; Composites

1. Introduction

Point-source Green's functions (GFs), referred as fundamental solutions, under homogeneous boundary conditions can be used to develop various analytical, semi-analytical and numerical computational schemes to solve boundary-value problems associated with the same physical law. The best-known schemes are the GF method (Mura, 1987) and the boundary element (BE) method (Brebbia et al., 1984). The GF method directly applies a point-source GF to solve the related problems under the same homogeneous boundary conditions, such as a classical inclusion problem. It results in an analytical or a semi-analytical method,

[☆] Publication of the National Institute of Standards and Technology, an agency of the US Government; not subject to copyright.

^{*} Corresponding author. Present address: Department of Mechanical and Aerospace Engineering, Florida Institute of Technology, Melbourne, FL 32901, USA. Tel.: +1-321-674-7713; fax: +1-321-674-8813.

E-mail address: boyang@fit.edu (B. Yang).

depending upon whether or not a numerical integration of the GF is involved. The BE method indirectly applies a point-source GF. It is developed based on a boundary-integral-equation formulation employing a point-source GF as its weighting function on the boundary quantities. A numerical treatment of the boundary-integral equation is required to solve the problems. The BE method can cope with arbitrary geometries and boundary conditions.

In the theory of linear elasticity, point-force GFs have been derived for infinite space, half-space, bimetals, trimaterials, and multilayers (e.g., Love, 1944; Mura, 1987; Ting, 1996; Pan and Yuan, 2000; Yang and Pan, 2002a,b, among others). These structures can be considered as a reference system and their point-force GFs be used to further develop the GFs of a point force or a force dipole in more complicated systems. Our objective is to derive the point-force GF of a heterogeneous solid based on a (given) reference GF. The target GF is called a defect GF since the target system is a system with “defect” changes of elastic stiffness upon the reference system. The defect GF can be used to develop the various computational schemes for the defect system. It is utilized in this work to derive the elastic field of eigenstrain in a generally heterogeneous anisotropic solid. The idea of deriving a defect GF based on a reference GF has been implemented within the Debye scalar model (Tewary, 2002) and within the lattice-statics theory (Tewary, 1973). In the previous lattice-statics case, an infinite perfect lattice structure was considered as the reference, and the corresponding reference lattice GF was called a perfect lattice GF. We develop here its continuum counterpart considering a rather general reference, which can be imperfect as well as the target system.

This paper is organized as follows. In Section 2, the continuum Dyson’s equation and defect GF are derived within the theory of anisotropic elasticity. In Section 3, the defect GF is applied to derive the elastic field of an eigenstrain field in a heterogeneous solid. In Section 4, the theory is reduced to a composite of inhomogeneous inclusions. Based on the Dyson’s equation, approximate schemes are proposed to efficiently solve the special case of slightly inhomogeneous inclusions. In Section 5, numerical results are reported for inhomogeneous inclusions in a half-space substrate to demonstrate the validity of the present formulation. Finally, conclusions are drawn in Section 6.

2. Continuum Dyson’s equation and defect Green’s function

We consider a heterogeneous, anisotropic, and linearly elastic body Ω , as shown in Fig. 1(a). A Cartesian frame, (x_1, x_2, x_3) is attached. The constitutive law is given by

$$\sigma_{ij}(\mathbf{x}) = C_{ijkl}^*(\mathbf{x})\varepsilon_{kl}(\mathbf{x}), \quad (1)$$

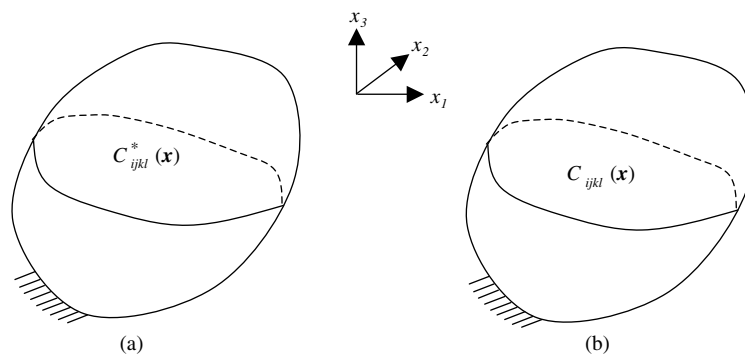


Fig. 1. (a) A heterogeneous solid $C_{ijkl}^*(\mathbf{x})$ under a homogeneous boundary condition and (b) a reference solid $C_{ijkl}(\mathbf{x})$ of the same geometry and under the same boundary condition as in (a).

where σ_{ij} is the stress component, $\varepsilon_{kl}(\equiv \frac{1}{2}(u_{k,l} + u_{l,k}))$ is the infinitesimal strain component, C_{ijkl}^* is the elastic stiffness component, and the repeated subscript implies the conventional summation over its range. In the definition of infinitesimal strain ε , \mathbf{u} is the displacement vector, and the comma in the subscript indicates the partial derivative with respect to the coordinate that follows. The body is subjected to a unit point force at \mathbf{X} along the p th direction. When the body is in equilibrium, the following equations are required:

$$\Sigma_{pij}^*(\mathbf{X}, \mathbf{x}) + \delta_{pi}\delta(\mathbf{x} - \mathbf{X}) = 0, \tag{2}$$

where $\Sigma_{pij}^*(\mathbf{X}, \mathbf{x})$ is the ij th stress component at \mathbf{x} when the unit point force is applied along the p th direction at \mathbf{X} , δ_{pi} is the Kronecker delta function, and $\delta(\mathbf{x} - \mathbf{X})$ is the Dirac delta function. Along $\partial\Omega$, the homogeneous boundary condition is prescribed, i.e., either displacement or traction in each component is prescribed to be equal to zero

$$G_{pi}^*(\mathbf{X}, \mathbf{x}) = 0 \quad \text{or} \quad \Sigma_{pij}^*(\mathbf{X}, \mathbf{x})n_j(\mathbf{x}) = 0, \quad \mathbf{x} \in \partial\Omega, \tag{3}$$

where $G_{pi}^*(\mathbf{X}, \mathbf{x})$ is the i th displacement component at \mathbf{x} when the unit point force is applied along the p th direction at source point \mathbf{X} , and $n_j(\mathbf{x})$ is the outward normal component at a (boundary) point \mathbf{X} . $G_{pi}^*(\mathbf{x}, \mathbf{x})$ is related to $\Sigma_{pij}^*(\mathbf{X}, \mathbf{x})$ through Hooke’s law, Eq. (1). Therefore, $G_{pi}^*(\mathbf{X}, \mathbf{x})$ and $\Sigma_{pij}^*(\mathbf{X}, \mathbf{x})$ are respectively the point-force Green’s displacement and stress of the system in Fig. 1(a) under the homogeneous boundary condition. Substituting Eq. (1) in Eq. (2) and applying the symmetry of C_{ijkl}^* result in

$$[C_{ijkl}^*(\mathbf{x})G_{pk,l}^*(\mathbf{X}, \mathbf{x})]_j + \delta_{pi}\delta(\mathbf{x} - \mathbf{X}) = 0. \tag{4}$$

For clarity, indices $p, q, s,$ and t are used to indicate a component of the source point (i.e., the first variable of the GFs), and indices $i, j, k,$ and l to indicate a component of the field point (i.e., the second variable of the GFs), through the text.

To solve the above Green’s problem, we now consider a reference body of elastic stiffness C_{ijkl} , generally heterogeneous as well, as shown in Fig. 1(b). The reference body has the same geometry (i.e., the same $\partial\Omega$) as the (target) body in Fig. 1(a). The difference of elastic stiffness between the reference and target bodies is given by

$$\Delta C_{ijkl}(\mathbf{x}) = C_{ijkl}(\mathbf{x}) - C_{ijkl}^*(\mathbf{x}). \tag{5}$$

The reference body is subjected to a point force f_i at \mathbf{x}_0 , and under the same homogeneous boundary condition as given in Eq. (2) for the target body

$$u_i(\mathbf{x}) = 0 \quad \text{or} \quad \sigma_{ij}(\mathbf{x})n_j(\mathbf{x}) = 0, \quad \mathbf{x} \in \partial\Omega. \tag{6}$$

The equilibrium of the reference body requires

$$[C_{ijkl}(\mathbf{x})u_{k,l}(\mathbf{x})]_j + f_i\delta(\mathbf{x} - \mathbf{x}_0) = 0. \tag{7}$$

We multiply Eq. (7) on its free index i with an arbitrary function $g_{pi}(\mathbf{X}, \mathbf{x})$ and integrate the product with respect to \mathbf{x} over the domain Ω

$$\int_{\Omega} g_{pi}(\mathbf{X}, \mathbf{x}') \{ [C_{ijkl}(\mathbf{x}')u_{k,l}(\mathbf{x}')]_j + f_i\delta(\mathbf{x}' - \mathbf{x}_0) \} dV(\mathbf{x}') = 0. \tag{8}$$

Applying the divergence theorem and realizing the property of the Dirac delta function yield

$$\int_{\partial\Omega} g_{pi}(\mathbf{X}, \mathbf{x}') C_{ijkl}(\mathbf{x}') u_{k,l}(\mathbf{x}') n_j(\mathbf{x}') dS(\mathbf{x}') - \int_{\Omega} g_{pi,j}(\mathbf{X}, \mathbf{x}') C_{ijkl}(\mathbf{x}') u_{k,l}(\mathbf{x}') dV(\mathbf{x}') + g_{pi}(\mathbf{X}, \mathbf{x}_0) f_i = 0. \tag{9}$$

Once again applying the divergence theorem yields

$$\int_{\partial\Omega} g_{pi}(\mathbf{X}, \mathbf{x}') C_{ijkl}(\mathbf{x}') u_{k,l}(\mathbf{x}') n_j(\mathbf{x}') dS(\mathbf{x}') - \int_{\partial\Omega} g_{pi,j}(\mathbf{X}, \mathbf{x}') C_{ijkl}(\mathbf{x}') u_k(\mathbf{x}') n_l(\mathbf{x}') dS(\mathbf{x}') + \int_{\Omega} [g_{pi,j}(\mathbf{X}, \mathbf{x}') C_{ijkl}(\mathbf{x}')],_l u_k(\mathbf{x}') dV(\mathbf{x}') + g_{pi}(\mathbf{X}, \mathbf{x}_0) f_i = 0. \tag{10}$$

Now, we let the weighting function $g_{pi}(\mathbf{X}, \mathbf{x})$ in Eqs. (8)–(10) be $G_{pi}(\mathbf{X}, \mathbf{x})$ that satisfies

$$[G_{pi,j}(\mathbf{X}, \mathbf{x}) C_{ijkl}(\mathbf{x})],_l + \delta_{pk} \delta(\mathbf{x} - \mathbf{X}) = 0, \tag{11}$$

$$G_{pi}(\mathbf{X}, \mathbf{x}) = 0 \quad \text{or} \quad \Sigma_{pij}(\mathbf{X}, \mathbf{x}) n_j(\mathbf{x}) = 0, \quad \mathbf{x} \in \partial\Omega, \tag{12}$$

where $\Sigma_{pij}(\mathbf{X}, \mathbf{x}) \equiv C_{ijkl}(\mathbf{x}) G_{pk,l}(\mathbf{X}, \mathbf{x})$. Eq. (12) gives the same homogeneous boundary conditions as given in Eqs. (2) and (6). Therefore, $G_{pi}(\mathbf{X}, \mathbf{x})$ and $\Sigma_{pij}(\mathbf{X}, \mathbf{x})$ are, respectively, the point-force Green’s displacement and stress of the reference body under the homogeneous boundary condition. Substituting Eqs. (6), (11) and (12) in Eq. (10) yields

$$u_p(\mathbf{X}) = G_{pi}(\mathbf{X}, \mathbf{x}_0) f_i. \tag{13}$$

Alternatively, we let the weighting function $g_{pi}(\mathbf{X}, \mathbf{x})$ in Eqs. (8)–(10) be $G_{pi}^*(\mathbf{X}, \mathbf{x})$ that satisfies Eqs. (3) and (4). Applying Eqs. (3) and (6) to Eq. (10) gives

$$\int_{\Omega} [G_{pi,j}^*(\mathbf{X}, \mathbf{x}') C_{ijkl}(\mathbf{x}')],_l u_k(\mathbf{x}') dV(\mathbf{x}') + G_{pi}^*(\mathbf{X}, \mathbf{x}_0) f_i = 0. \tag{14}$$

Applying Eq. (5) and then Eq. (3), and rearranging result in

$$u_p(\mathbf{X}) = \int_{\Omega} [G_{pi,j}^*(\mathbf{X}, \mathbf{x}') \Delta C_{ijkl}(\mathbf{x}')],_l u_k(\mathbf{x}') dV(\mathbf{x}') + G_{pi}^*(\mathbf{X}, \mathbf{x}_0) f_i. \tag{15}$$

Although different weighting functions are applied, $\mathbf{u}(\mathbf{X})$ in Eqs. (13) and (15) must be the same (unique) solution to Eqs. (6) and (7). Thus, Eq. (13) is applied to Eq. (15), leading to

$$G_{pi}(\mathbf{X}, \mathbf{x}_0) f_i = \int_{\Omega} [G_{pk,j}^*(\mathbf{X}, \mathbf{x}') \Delta C_{jkst}(\mathbf{x}')],_t G_{si}(\mathbf{x}', \mathbf{x}_0) f_i dV(\mathbf{x}') + G_{pi}^*(\mathbf{X}, \mathbf{x}_0) f_i. \tag{16}$$

Because the vector f_i and its location 0_x are arbitrary, we finally have

$$G_{pi}^*(\mathbf{X}, \mathbf{x}) = G_{pi}(\mathbf{X}, \mathbf{x}) - \int_{\Omega} [G_{pk,j}^*(\mathbf{X}, \mathbf{x}') \Delta C_{jkst}(\mathbf{x}')],_t G_{si}(\mathbf{x}', \mathbf{x}) dV(\mathbf{x}'). \tag{17}$$

Equation (17) provides an integral-equation linkage between the GF \mathbf{G}^* of the target body in Fig. 1(a) and the GF \mathbf{G} of the reference body in Fig. 1(b). It is the continuum counterpart of the lattice-statics Dyson’s equation in the lattice theory of defect GF provided that the elastic constants can be related to the force constants in the lattice theory (Maradudin et al., 1971; Tewary, 1973). $\Delta\mathbf{C}$ corresponds to the difference of force constants in the defect lattice space. \mathbf{G}^* and \mathbf{G} correspond respectively to the defect and perfect lattice GFs. Thus, we call Eq. (17) the continuum Dyson’s equation, \mathbf{G}^* the defect GF, and \mathbf{G} the reference GF. In the lattice theory, the original Dyson’s equation takes the perfect lattice as the reference lattice. It can obviously be generalized by taking an arbitrary lattice in place of the perfect lattice as the reference. Consequently, a complete correspondence between the continuum and lattice Dyson’s equations can be established. These equations link, respectively, on the continuum and lattice levels, the point-force responses of two systems of identical geometry and (homogeneous) boundary conditions but of different media. Based on the formulation on either level, given the GF of either system (called here a reference), the GF of the other (called here a target or defect system with “defect” change of materials property relative to the reference) can be obtained by solving the corresponding Dyson’s equation within the defect space.

3. Defect Green’s function formulation of eigenstrain (eigenstress)

Now, we consider the body in Fig. 1(a) that contains an eigenstrain field under the same homogeneous boundary condition as given in Eq. (3). The constitutive law is given by

$$\sigma_{ij} = C_{ijkl}^*(\varepsilon_{kl} - \varepsilon_{kl}^0) \quad \text{or} \quad \sigma_{ij} = C_{ijkl}^*\varepsilon_{kl} - \sigma_{ij}^0, \tag{18}$$

where ε_{kl}^0 is the eigenstrain, and $\sigma_{ij}^0 (\equiv C_{ijkl}^*\varepsilon_{kl}^0)$ is the corresponding eigenstress. The equilibrium equations are given by

$$[C_{ijkl}^*(\mathbf{x})u_{k,l}(\mathbf{x}) - \sigma_{ij}^0]_{,j} = 0. \tag{19}$$

The boundary conditions are given by

$$u_i(\mathbf{x}) = 0 \quad \text{or} \quad \sigma_{ij}(\mathbf{x})n_j(\mathbf{x}) = 0, \quad \mathbf{x} \in \partial\Omega. \tag{20}$$

We multiply Eq. (19) on its free index i with the defect GF $G_{pi}^*(\mathbf{X}, \mathbf{x})$ and integrate the product over the domain Ω . Following the same procedure from Eqs. (8)–(10) and applying the homogeneous boundary conditions in Eqs. (3) and (20), we obtain

$$u_p(\mathbf{X}) = - \int_{\Omega} G_{pi}^*(\mathbf{X}, \mathbf{x})\sigma_{ij,j}^0(\mathbf{x}) dV(\mathbf{x}). \tag{21}$$

Taking derivatives of Eq. (21) and applying the definition of strain ε result in

$$\varepsilon_{pq}(\mathbf{X}) = - \int_{\Omega} \frac{1}{2} [G_{pi,q}^*(\mathbf{X}, \mathbf{x}) + G_{qi,p}^*(\mathbf{X}, \mathbf{x})]\sigma_{ij,j}^0(\mathbf{x}) dV(\mathbf{x}). \tag{22}$$

Consequently, by applying the Hooke’s law, Eq. (18), the stress σ is given by

$$\sigma_{pq}(\mathbf{X}) = -C_{pqst}^*(\mathbf{X}) \int_{\Omega} G_{si,t}^*(\mathbf{X}, \mathbf{x})\sigma_{ij,j}^0(\mathbf{x}) dV(\mathbf{x}) - \sigma_{pq}^0(\mathbf{X}). \tag{23}$$

Therefore, once the defect GF \mathbf{G}^* and its derivatives that satisfy Eqs. (2) and (3) are available, the problem of eigenstrain in a heterogeneous solid under the homogeneous boundary conditions can be solved.

4. Application to composite of inhomogeneous inclusions

The derivation in previous sections has been general, treating an arbitrary heterogeneous target body and an arbitrary heterogeneous reference matrix. The resulting continuum Dyson’s equation (17) is given in a general volume-integral form relating the defect and reference GFs. The integral involves the stiffness difference, $\Delta\mathbf{C}$. Generally speaking, one can manage on this equation to develop an implicit algorithm for evaluating the defect GF by numerically discretizing the domain where the stiffness difference $\Delta\mathbf{C}$ is nontrivial. However, the resulting system of algebraic equations has in general a full stiffness matrix. If the nontrivial $\Delta\mathbf{C}$ spans a large space, this way of solving the problem of a heterogeneous solid is computationally inefficient, for instance, compared to a finite-element method involving a sparse stiffness matrix. Nonetheless, the continuum Dyson’s equation (10) may find useful application in certain cases, for instance, in the case that the stiffness difference $\Delta\mathbf{C}$ is localized in small regions (i.e., small defect space). In this case, only those small regions of nontrivial $\Delta\mathbf{C}$ need to be numerically discretized. Further, if the stiffness difference $\Delta\mathbf{C}$ is small, an explicit expression of the defect GF can be obtained by approximating the Dyson’s equation.

Let us consider a particular heterogeneous solid of multiple particles embedded in a reference matrix, as shown in Fig. 2. The particles and matrix are perfectly bonded. Because these particles are inhomogeneous

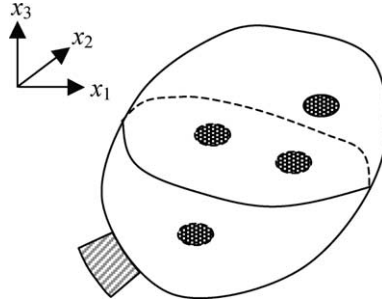


Fig. 2. A composite of inhomogeneous inclusions (shadowed spots).

relative to the matrix and contain eigenstrains, they are called inhomogeneous inclusions, following Mura's terminology (Mura, 1987). This composite may represent a particle-reinforced polymer-matrix composite (Lee and Mykkanen, 1987) and a semiconductor matrix with buried quantum dots (Bimberg et al., 1998). The reference matrix may itself be heterogeneous, for example, a multilayered structure, such as composite laminates and semiconductor superlattice across a wide range of length scales. In this case, the regions of nontrivial stiffness difference and the regions of nontrivial eigenstrain are matched. However, this match is not required in the earlier general formulation.

Applying the divergence theorem, we rewrite Eq. (21) as

$$u_p(\mathbf{X}) = \int_{\Omega} G_{pi,j}^*(\mathbf{X}, \mathbf{x}) \sigma_{ij}^0(\mathbf{x}) dV(\mathbf{x}) - \int_{\partial\Omega} G_{pi}^*(\mathbf{X}, \mathbf{x}) \sigma_{ij}^0(\mathbf{x}) n_j(\mathbf{x}) dS(\mathbf{x}). \quad (24)$$

By realizing that the eigenstress is localized inside the particles, the second term of surface integral is eliminated. Also, the first term of volume integral is reduced to the subdomains $\Omega^{(n)}$ of the particles. That is

$$u_p(\mathbf{X}) = \sum_{n=1}^N \int_{\Omega^{(n)}} G_{pi,j}^*(\mathbf{X}, \mathbf{x}) \sigma_{ij}^0(\mathbf{x}) dV(\mathbf{x}), \quad (25)$$

where N is the total number of particles. The strain ε and stress σ are thus given by

$$\varepsilon_{pq}(\mathbf{X}) = \sum_{n=1}^N \int_{\Omega^{(n)}} \frac{1}{2} [G_{pi,jq}^*(\mathbf{X}, \mathbf{x}) + G_{qi,jp}^*(\mathbf{X}, \mathbf{x})] \sigma_{ij}^0(\mathbf{x}) dV(\mathbf{x}), \quad (26)$$

$$\sigma_{pq}(\mathbf{X}) = C_{pqst}^*(\mathbf{x}) \sum_{n=1}^N \int_{\Omega^{(n)}} G_{si,jt}^*(\mathbf{X}, \mathbf{x}) \sigma_{ij}^0(\mathbf{x}) dV(\mathbf{x}) - \sigma_{pq}^0(\mathbf{x}). \quad (27)$$

Further, we can reduce Eqs. (25)–(27) to a surface integral for those particles whose eigenstress is uniform. Without loss of generality, we assume that all the particles hold a uniform eigenstress. Once again applying the divergence theorem yields

$$u_p(\mathbf{X}) = \sum_{n=1}^N \sigma_{ij}^{0(n)} \int_{\partial\Omega^{(n)}} G_{pi}^*(\mathbf{X}, \mathbf{x}) n_j(\mathbf{x}) dS(\mathbf{x}), \quad (28)$$

where $\sigma_{ij}^{0(n)}$ is the (uniform) eigenstress in the n th particle, and $\partial\Omega^{(n)}$ is its boundary (i.e., interface with the matrix). Eqs. (26) and (27) are reduced to

$$\varepsilon_{pq}(\mathbf{X}) = \sum_{n=1}^N \sigma_{ij}^{0(n)} \int_{\partial\Omega^{(n)}} \frac{1}{2} [G_{pi,q}^*(\mathbf{X}, \mathbf{x}) + G_{qi,p}^*(\mathbf{X}, \mathbf{x})] n_j(\mathbf{x}) dS(\mathbf{x}), \quad (29)$$

$$\sigma_{pq}(\mathbf{X}) = C_{pqst}^*(\mathbf{x}) \sum_{n=1}^N \sigma_{ij}^{0(n)} \int_{\partial\Omega^{(n)}} G_{si,t}^*(\mathbf{X}, \mathbf{x}) n_j(\mathbf{x}) dS(\mathbf{x}) - \sigma_{pq}^0(\mathbf{X}). \quad (30)$$

Now, applying the divergence theorem and realizing that ΔC is localized inside the particles, we reduce the expression of the defect GF, Eq. (17), to

$$G_{pi}^*(\mathbf{X}, \mathbf{x}) = G_{pi}(\mathbf{X}, \mathbf{x}) + \sum_{n=1}^N \int_{\Omega^{(n)}} G_{pk,j}^*(\mathbf{X}, \mathbf{x}') \Delta C_{jkst}(\mathbf{x}') G_{si,t}(\mathbf{x}', \mathbf{x}) dV(\mathbf{x}'). \quad (31)$$

Let us insert the above Dyson's expression of the defect GF into its integrant repeatedly. Consequently, we obtain a series expression of the defect GF. Assuming that ΔC is small compared to both C and C^* , we can approximate the defect GF by

$$G_{pi}^*(\mathbf{X}, \mathbf{x}) = G_{pi}(\mathbf{X}, \mathbf{x}) + o(\Delta C), \quad (32)$$

on the zeroth-order, and approximate it by

$$G_{pi}^*(\mathbf{X}, \mathbf{x}) = G_{pi}(\mathbf{X}, \mathbf{x}) + \sum_{n=1}^N \int_{\Omega^{(n)}} G_{pk,j}(\mathbf{X}, \mathbf{x}') \Delta C_{jkst}(\mathbf{x}') G_{si,t}(\mathbf{x}', \mathbf{x}) dV(\mathbf{x}') + o(\Delta C^2), \quad (33)$$

on the first-order. Eq. (32) is accurate on the order of $o(\Delta C)$ while Eq. (33) is accurate on the order of $o(\Delta C^2)$. In a similar way, Flinn and Maradudin (1962) expanded the lattice Dyson's equation and truncated the series expression to approximately evaluate the defect lattice GF. These approximate but explicit expressions are used next to evaluate the elastic field of slightly inhomogeneous inclusions in a reference half-space matrix.

5. Numerical results

We now apply the theory developed in previous sections to examine the elastic field in a semi-infinite GaAs substrate due to inhomogeneous inclusions. The homogeneous half-space substrate is considered as the reference system. The three independent elastic constants of the (cubic) GaAs substrate are given by $C_{11} = 118$ GPa, $C_{12} = 54$ GPa, and $C_{44} = 59$ GPa in its crystallographic base axes. One may refer to Ting (1996) for how to construct the full stiffness matrix C_{ijkl} . The elastic constants of the inhomogeneous inclusions are taken to be proportional to those of the substrate: $C_{ijkl}^* = (1 - \lambda)C_{ijkl}$. The x_3 -axis of the coordinate system is set to be perpendicular to the free surface and pointing to the interior of the substrate. The crystallographic base axes $[100]$, $[010]$ and $[001]$ are parallel respectively to each of the global coordinates (x_1, x_2, x_3) . The shape of the inhomogeneous inclusions is taken to be cuboidal with dimensions $a \times a \times a/2$. The sides of the inhomogeneous inclusions are parallel to the global coordinates. The eigen-strain in the inhomogeneous inclusions is hydrostatic, i.e., $\varepsilon_{ij}^0 = \varepsilon^0 \delta_{ij}$, and is uniform in each inclusion. The scheme developed by Pan and Yuan (2000) is adopted to evaluate the reference GF of the semi-infinite anisotropic elastic solid.

We consider an array of three inhomogeneous inclusions aligned in the (100) direction inside the GaAs substrate, as shown in Fig. 3. The depth from the center of the inhomogeneous inclusions to the substrate surface is indicated by h . The spacing of the inhomogeneous inclusions is set to be $2a$. The induced elastic field is solved by applying Eqs. (25)–(27). However, the defect GF, G^* is evaluated approximately on the zeroth-order by using Eq. (32) and on the first-order by using Eq. (33). The complete solution is also obtained for comparison by using a numerical BE method (Yang and Pan, 2002c). The BE solution adopted for the comparison has acclaimed a convergence of 1% by doubling the mesh density in either dimension. Results of these simulations are plotted in Figs. 4 and 5.

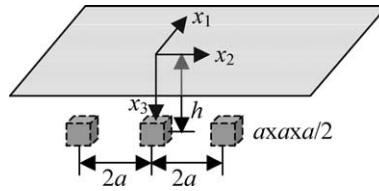


Fig. 3. A semi-infinite substrate with three inhomogeneous inclusions at depth h .

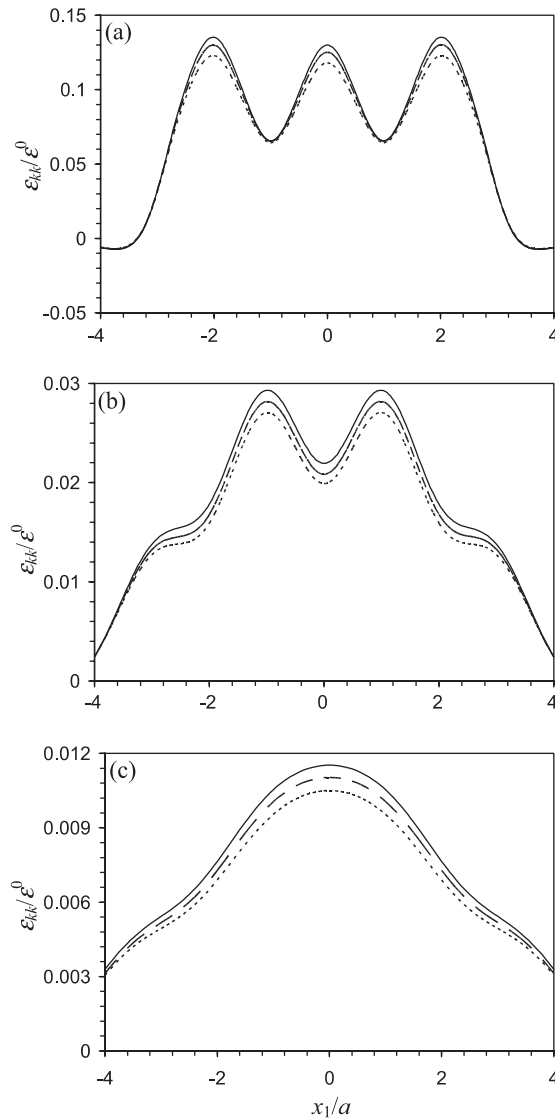


Fig. 4. Variations of normalized hydrostatic strain $\varepsilon_{kk}/\varepsilon^0$ along a line $(x_1, 0, 0)$ over three inhomogeneous inclusions buried at different depths in a half-space substrate: (a) $h = a$; (b) $h = 2a$; (c) $h = 3a$, solved by the BE method (solid), by the GF method in the first-order approximation (dashed), and by the GF method in the zeroth-order approximation (dotted).

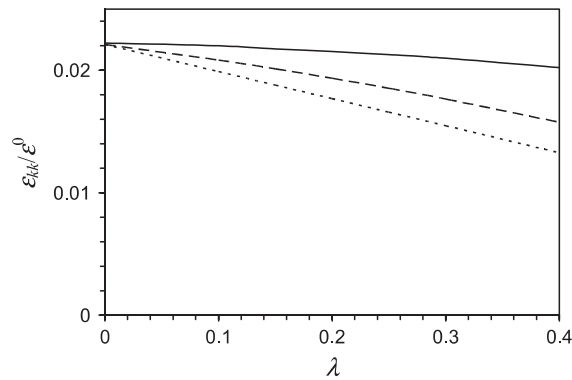


Fig. 5. Variations of normalized hydrostatic strain $\varepsilon_{kk}/\varepsilon^0$ with mismatch factor λ at $(0, 0, 0)$ over three inhomogeneous inclusions buried at depth $h = 2a$ in a half-space substrate, solved by the BE method (solid), by the GF method in the first-order approximation (dashed), and by the GF method in the zeroth-order approximation (dotted).

Fig. 4 shows the variation of normalized hydrostatic strain $\varepsilon_{kk}/\varepsilon^0$ along a line $(x_1, 0, 0)$ on the surface at a fixed stiffness mismatch factor $\lambda = 0.1$ in three cases with $h = a, 2a$, and $3a$, respectively. In all these cases, the first-order approximate solution is closer to the BE complete solution than the zeroth-order approximate solution. The relative error in the zeroth-order approximate solution (at location $(0, 0, 0)$ of the maximum error) is about 9% compared to the mismatch factor λ of 0.1. The relative error in the first-order approximate solution at the same location is about 4%, appreciably smaller than the former. The profiles of the elastic response to the three inhomogeneous inclusions viewed on the top surface show an interesting transition with depth h . At $h = a$, there appear to be three hills in the induced hydrostatic strain field. Their peaks are nearly right above the centers of the three inhomogeneous inclusions. At $h = 2a$, the number of hills is reduced to two. Their peaks are between the central and the side inclusions. At $h = 3a$, the number of hills is further reduced to one. Its peak is right above the center of the central inclusion. Therefore, one would observe on the top surface one, two, and three “images” of the three finite-size inhomogeneous inclusions, depending upon their depth under the surface. The magnitude of the normalized hydrostatic strain on the surface is reduced by about one order when the depth of the inclusions varies from $h = a$ to $3a$.

Fig. 5 shows the variation of normalized hydrostatic strain $\varepsilon_{kk}/\varepsilon^0$ at a fixed point $(0, 0, 0)$ with stiffness-mismatch factor λ . The depth of the inhomogeneous inclusions, h , is fixed at $2a$. The variations of $\varepsilon_{kk}/\varepsilon^0$ with λ at $h = a$ and $3a$ are similar. At $\lambda = 0$, all the solutions by the BE method and the zeroth- and first-order approximate schemes are identical (within the computation accuracy), as expected. They depart from each other as λ increases. The deviation of the zero-order approximate solution from the BE solution is nearly linear. Meanwhile, the deviation of the first-order approximate solution from the BE solution stays on the order of λ^2 but does not follow closely the quadratic rate.

6. Conclusions

We have introduced the continuum Dyson’s equation and defect Green’s function for heterogeneous, anisotropic, and linearly elastic solids under homogeneous boundary conditions. The continuum Dyson’s equation is the counterpart of the lattice Dyson’s equation in the lattice theory, relating the Green’s responses of two systems of identical geometry and boundary condition but of different media. Given the reference GF, the defect GF can be obtained by solving the Dyson’s equation. The defect GF is applied to solve the problem of eigenstrain in a generally heterogeneous anisotropic solid. In particular, a composite

consisting of inhomogeneous inclusions is examined in detail. Approximate computational schemes have been proposed to efficiently evaluate the elastic field of slightly inhomogeneous inclusions. Numerical results of three inhomogeneous inclusions in a semi-infinite GaAs substrate with a traction-free surface were reported to demonstrate the validity of the present formulation. It was observed that the number of “images” of the three inclusions seen on the top surface undergoes a transition from one to three with the depth of inclusions as the parameter.

Acknowledgements

BY acknowledges the financial support from Kent State University and Massachusetts Institute of Technology through the NSF project #0121545.

References

- Bimberg, D., Grundmann, M., Ledentsov, N.N., 1998. *Quantum Dot Heterostructures*. John Wiley and Sons Ltd., New York.
- Brebbia, C.A., Telles, J.C.F., Wrobel, L.C., 1984. *Boundary Element Techniques: Theory and Applications in Engineering*. Springer-Verlag, Berlin.
- Flinn, P.A., Maradudin, A.A., 1962. *Annual Physics* 18, 81.
- Lee, J.A., Mykkanen, D.L., 1987. *Metal and Polymer Matrix Composites*. Noyes Data Corp., Park Ridge, NJ.
- Love, A.E.H., 1944. *A Treatise on the Mathematical Theory of Elasticity*. Dover, New York.
- Maradudin, A.A., Montroll, E.W., Weiss, G.H., Ipatova, I.P., 1971. *Theory of Lattice Dynamics in the Harmonic Approximation*. Academic Press, New York, London.
- Mura, T., 1987. *Micromechanics of Defects in Solids*. Martinus Nijhoff, Boston.
- Pan, E., Yuan, F.G., 2000. Three-dimensional Green's functions in anisotropic bimetals. *International Journal of Solids and Structures* 37, 5329.
- Tewary, V.K., 1973. Green-function method for lattice statics. *Advances in Physics* 22, 757.
- Tewary, V.K., 2002. Change in low-temperature thermodynamic functions of a semiconductor due to a quantum dot. *Physical Review B* 66, 205321.
- Ting, T.C.T., 1996. *Anisotropic Elasticity*. Oxford University Press, Oxford.
- Yang, B., Pan, E., 2002a. Three-dimensional Green's functions in anisotropic trimetals. *International Journal of Solids and Structures* 39, 2235.
- Yang, B., Pan, E., 2002b. Efficient evaluation of three-dimensional Green's functions in anisotropic elastostatic multilayered composites. *Engineering Analysis with Boundary Elements* 26, 355.
- Yang, B., Pan, E., 2002c. Elastic analysis of an inhomogeneous quantum dot in multilayered semiconductors using a boundary element method. *Journal of Applied Physics* 92, 3084.